Photoluminescence spectroscopy of HgCdTe quantum well heterostructures in the $15-30\,\mu$m wavelength range

© V.V. Rumyantsev[1,2], A.A. Razova[1,2], D.V. Kozlov[1,2], M.A. Fadeev[1], K.V. Maremyanin[1], V.V. Utochkin[1], N.N. Mikhailov[3], S.A. Dvoretsky[3], V.I. Gavrilenko[1,2], S.V. Morozov[1,2]

[1] Institute of Physics of Microstructures, Russian Academy of Sciences,
603950 Nizhny Novgorod, Russia
[2] Lobachevsky State University of Nizhny Novgorod,
603950 Nizhny Novgorod, Russia
[3] Rzhanov Institute of Semiconductor Physics, Siberian Branch, Russian Academy of Sciences,
630090 Novosibirsk, Russia

E-mail: rumyantsev@ipm.sci-nnov.ru

Received December 25, 2021
Revised December 30, 2021
Accepted December 30, 2021

In recent years, narrow gap heterostructures with $Hg_{1-x}Cd_xTe/Cd_yHg_{1-y}Te$ quantum wells have been actively studied both in connection with the topic of topological insulators and from the point of view of their application in optoelectronics in the terahertz domain. In this work, we study the photoconductivity and photoluminescence spectra of structure with a band gap of 40 meV. In addition to interband transitions, the features of the spectra associated with the resonance states of acceptors have been identified. The possibilities of using the structures under study to develop interband emitters at a wavelength of $\sim 30\,\mu$m, which is inaccessible to existing quantum-cascade lasers, are discussed.

Keywords: narrow-gap semiconductors, HgCdTe, resonance states, acceptors, photoluminescence.

DOI: 10.21883/SC.2022.05.53425.9790

1. Introduction

In recent years, narrow gap heterostructures with $Hg_{1-x}Cd_xTe/Cd_yHg_{1-y}Te$ quantum wells (QWs) have been actively studied both in connection with the topic of topological insulators [1–4], and from the point of view of their application in optoelectronics in the terahertz domain [5]. In particular, QWs based on HgCdTe can be used as the active medium for long-wavelength lasers based on interband transitions, which can compete with quantum-cascade lasers (QCLs). This is especially topical in the wavelength range of $20-60\,\mu$m, which, due to strong lattice absorption in materials $A^{III}B^{V}$ used to create QCLs, today remains practically not covered by them [6,7]. It is assumed that the quantum efficiency of interband photoluminescence (PL) and stimulated emission (SE) of structures with Hg(Cd)Te/CdHgTe QWs at the same band gap depends on the carrier-dispersion law [8,9], the form of which is determined by the parameters (thickness and proportion of cadmium in the QW, as well as the composition of the barriers).

Knowing the QW parameters, one can use numerical methods to estimate the efficiency of Auger recombination, which is one of the main factors hindering the production of long-wavelength SE. As was shown in the works [9,10], the efficiency of Auger recombination correlates with the value of the so-called threshold energy of the Auger process, which is uniquely determined by the band spectrum of the structure under study. The threshold energy is defined as the minimum kinetic energy, in which case a system of three particles can participate in the Auger process [11]. The determination of the efficiency of Auger recombination is most important in the wavelength range in the vicinity of $30\,\mu$m and more, where, due to the growing phonon absorption [12] and absorption on free carriers, the high concentration of carriers is required to obtain amplification, which bring on the increase in rate of Auger recombination.

Modern molecular beam epitaxy (MBE) technology makes it possible to grow high-quality structures with *in situ* ellipsometric control of parameters [13,14]. However, accurate determination of the Cd concentration in layers several nanometers in thickness for this method is still a relatively difficult task. The alternative way to refine the structure parameters is detailed measurements of the photoconductivity (PC) and PL spectra. In addition to interband transitions, the PL and PC spectra also provide information on transitions associated with the presence of impurities and defects in the material. The study of transitions involving impurities is most relevant for radiation receivers, since impurity levels lead to nonradiative Shockley–Read–Hall recombination [15–18], however, impurity transitions also affect the characteristics of low-power radiating sources. One of the most common point imperfections in HgCdTe-based structures is the mercury vacancy, which is the divalent acceptor [19,20]. It can be in three charge states: the neutral A_2^0-center, the partially ionized A_2^{-1}-center, and fully ionized A_2^{-2}-center [21]. In narrow-bandgap heterostructures, acceptor centers can appear in the conduction band, which will lead to the formation of so-called resonance states, the description

and identification of which is the separate interesting problem.

In this work, an experimental study of the PC and PL spectra on the basis of which the *ex situ* characterization of the structure designed for the generation of long-wavelength radiation in the vicinity of 30 μm is carried out. Based on the refined parameters, the threshold energy of Auger recombination is estimated for the structure under study, and the possibilities of obtaining SE on interband transitions are discussed. In addition to interband transitions, features associated with transitions between the valence band continuum and the resonance state of acceptor were found for the first time in the PL spectra.

2. Examined samples and experimental procedure

In this work, the waveguide heterostructure with Hg(Cd)Te/CdHgTe quantum wells, grown in the ISP SB RAS by the MBE-method on a semi-insulating GaAs substrate in the growth direction [013] using ZnTe and CdTe buffer layers [22], is studied. The array (10 QWs) of HgCdTe quantum wells separated by wide-band CdHgTe light-blocking layers, which are the active region of the structures, is placed in waveguide layers. The active area is located at the antinode of the TE_0-mode, localization of which occurs due to the gradient of the refractive index between the waveguide layers and between the waveguide layers and air [10].

To study the photoconductivity spectra, the samples were placed at the end of waveguide insert, which was placed in the Dewar vessel with liquid helium or liquid nitrogen. Radiation was supplied from a Bruker Vertex 80v Fourier spectrometer evacuated to pressure of 10^{-3} bar, where the globar was used as the radiation source. When measuring the PC spectra, depending on the range, beamsplitters based on Mylar and potassium bromide were used, as well as a KRS5 filter to separate the evacuated part of the spectrometer from the area filled with liquid helium or nitrogen.

When studying the PL and PC spectra, the samples were placed in the closed-cycle helium cryostat providing temperature control in the range from 8 to 300 K. As a source of excitation in the study of FL the current-wave diode laser with operating wavelength of 808 nm and characteristic power of 100 mW was used. The spectra were recorded using the Fourier spectrometer optically coupled to the cryostat and operating in the step-by-step scanning mode [23]. Silicon bolometer was used as the radiation detector.

To determine the parameters of the structures, the experimental data were compared with the results of theoretical calculations performed within the framework of the Bert–Foreman model with the Kane Hamiltonian 8×8 with temperature-dependent parameters [24]. The threshold energy of Auger recombination was determined by the technique for finding the extrema [25]. The calculation of the ionization energy of the mercury vacancy was carried out by a method that takes into account the chemical shift and the effect of „charge-images“ arising due to different dielectric permittivities of the heterostructure layers. The method used is described in more detail in [26].

3. Studies of photoconductivity and photoluminescence

Figure 1 shows the PC spectra of the structure under study, obtained at temperatures of 4.2 and 77 K. Both spectra have a sharp long-wave edge corresponding to transitions between the main subzones of dimensional quantization ($v1-c1$). Higher in energy, in the 250 meV region, the peak is observed that corresponds to the energy of transition between the second valence sub-band and the second sub-band in the conduction band ($v2-c2$). At the temperature of 77 K, the second PC peak partially overlaps with a dip in the range of 280–300 meV, which is associated with absorption in liquid nitrogen. With temperature increase, both observed transitions shift towards shorter wavelengths, which confirms the normal band structure in the QW. In this case, the temperature shift of the $v2-c2$ transitions is less pronounced. This is due to the weaker temperature dependence of the extrema of the $c2$ and $v2$ sub-bands due to the greater distance in energy from the „bottom“ of the QW. Due to the thick waveguide layers, the use of contacts for transport measurements was difficult. To estimate the Burstein–Moss shift, the dark carrier concentration was estimated in terms of area of the cyclotron resonance curve. For the structure under study, it was $2.5 \cdot 10^{10}$ cm^{-2}.

The shift in the energy of the observed transitions with increasing temperature makes it possible to correct the structure parameters obtained from *in situ* ellipsometry

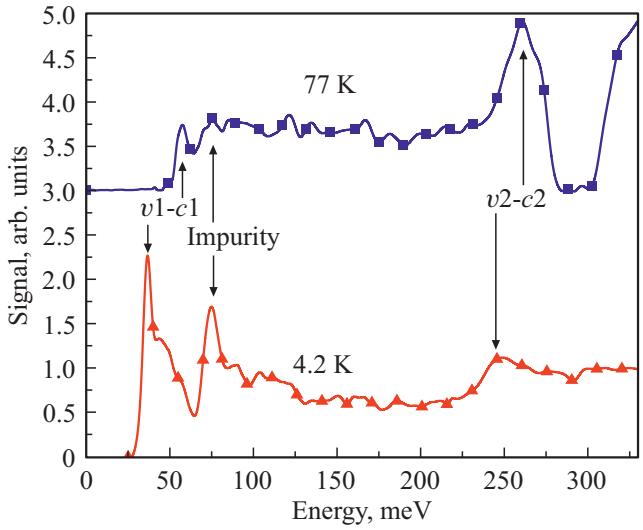

Figure 1. Photoconductivity spectra of the structure under study, measured at temperatures of 4.2 and 77 K.

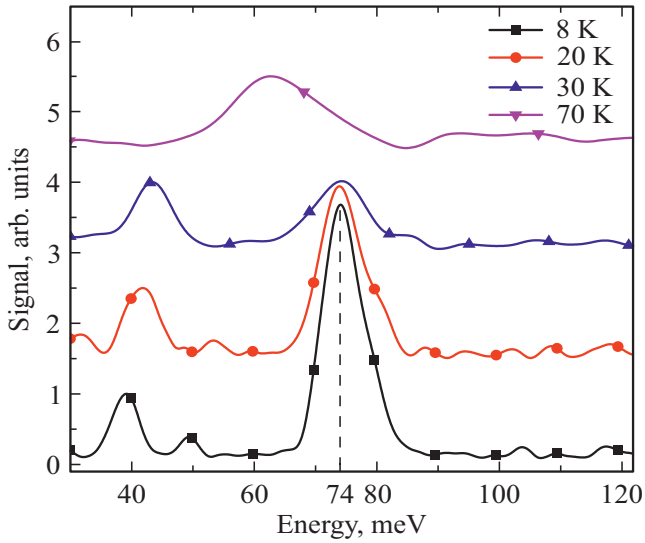

Figure 2. Normalized stationary photoluminescence spectra at various temperatures.

data, since the temperature change in the transition energy depends on both the QW width and the cadmium content in it. By fitting the QW parameters used to calculate the band gap in the $Hg_{-x}Cd_xTe/Hg_{1-y}Cd_yTe$ QW (transition $v1-c1$) for two different temperatures, it is possible to uniquely determine the unknown parameters, i.e. the width of the well and the content of cadmium in it. Similar calculations can be made for the transition energies $v2-c2$ or by comparing the transition energies of the ground and excited states at the same temperature. In this case, the greatest accuracy is achieved when comparing the transition energies $v1-c1$ and $v2-c2$, since in this case the dependence on the well parameters is the sharpest. In addition, the presence of excited transitions in the PC spectra can be useful for characterizing structures with a smaller band gap, for which the interband transition boundary will be superimposed on the features of the PC spectra associated, for example, with the band of residual rays in the GaAs substrate.

The best agreement between the observed PC pattern and the calculation results is achieved at the parameter value $c_{Cd} = 0.102$, $d = 11$ nm. In this case, the energies of both transitions between the ground and excited states correspond to the PC spectra. The high content of Cd in the QW, as well as the use of relatively narrow-bandgap barriers ($x_{Cd} = 0.58$), leads to the fact that the threshold Auger recombination is only 8 meV, which is practically 2 times less than in the structure described in the work [10].

On the PL spectra measured at temperatures from 10 to 70 K and shown in Fig. 2, one can see two lines: the long-wavelength line, corresponding to photon energies ~ 37 meV, and the short-wavelength one, corresponding to the energy of 74 meV. The first line corresponds with good accuracy to the position of „the red boundary“ of PC (i.e., the photon energy in this line corresponds to the difference between the energies of the edges of the lower electron sub-band and the upper hole sub-band) and shifts to the short-wavelength region with increasing temperature, so it is natural to relate it with interband transitions. The position of the second, shorter-wavelength PL line also coincides with a good accuracy with the ~ 75 meV feature in the PC spectrum and does not change with temperature increase. The intensity of this PL line rapidly decreases with temperature, and it becomes poorly distinguishable in the PL spectra at $T > 50$ K. It should be noted, however, that the ~ 75 meV feature in the PC spectrum is also noticeable at 77 K, although it is weakly expressed. This feature of the PC and PL spectra is associated with transitions whose energy practically does not change with temperature, i.e., it cannot be related to interband transitions. The feature at 75 meV can be associated with transitions between one of the bands and the impurity/defect state associated with the same band. Since the effective electron mass in narrow-bandgap HgCdTe solid-state solutions is very small, the binding energy ~ 75 meV can only correspond to acceptor centers.

Please note that the HgCdTe material always contains at least doubly charged acceptors formed by mercury vacancies arising due to the weak chemical bonding of Hg–Te. Nevertheless, the corresponding PL and PC lines observed in this work require more detailed consideration, since they are above the edge of interband transitions in energy. This distinguishes them from the typical case when the observed features of the spectra are associated with transitions between states of the continuous spectrum and localized states located in the band gap. In our case, the acceptor states are, in all probability, resonant, i.e. fall within the conduction band continuum. Such states have previously been observed only in the PC spectra of volume HgCdTe films [27].

4. Analysis of transitions associated with resonance states of acceptors

Before turning to the interpretation of the observed features of the spectra, let us describe the states of the acceptor centers present in the sample under study. Mercury vacancy is the divalent acceptor that can be in three charge states: neutral A_2^0-center, partially ionized A_2^{-1}-center and fully ionized A_2^{-2}-center [21]. In this case, the observed quantities are the ionization energies A_2^0- and A_2^{-1}-centers, which we denote as E_0 and E_1 respectively.

Figure 3, *a* shows the calculated ionization energy of a partially ionized mercury vacancy (E_1) at different positions of the acceptor center in the heterostructure quantum well. The calculation was carried out by the method that takes into account the chemical shift and the effect of „charge-images“ arising from different permittivities of the heterostructure layers. The method is described in detail in the work [26]. As can be seen from Fig. 3, *a*, the binding energy of the A_2^{-1}-center at the center of the QW is 75.6 meV, i.e., the state of such center falls within the

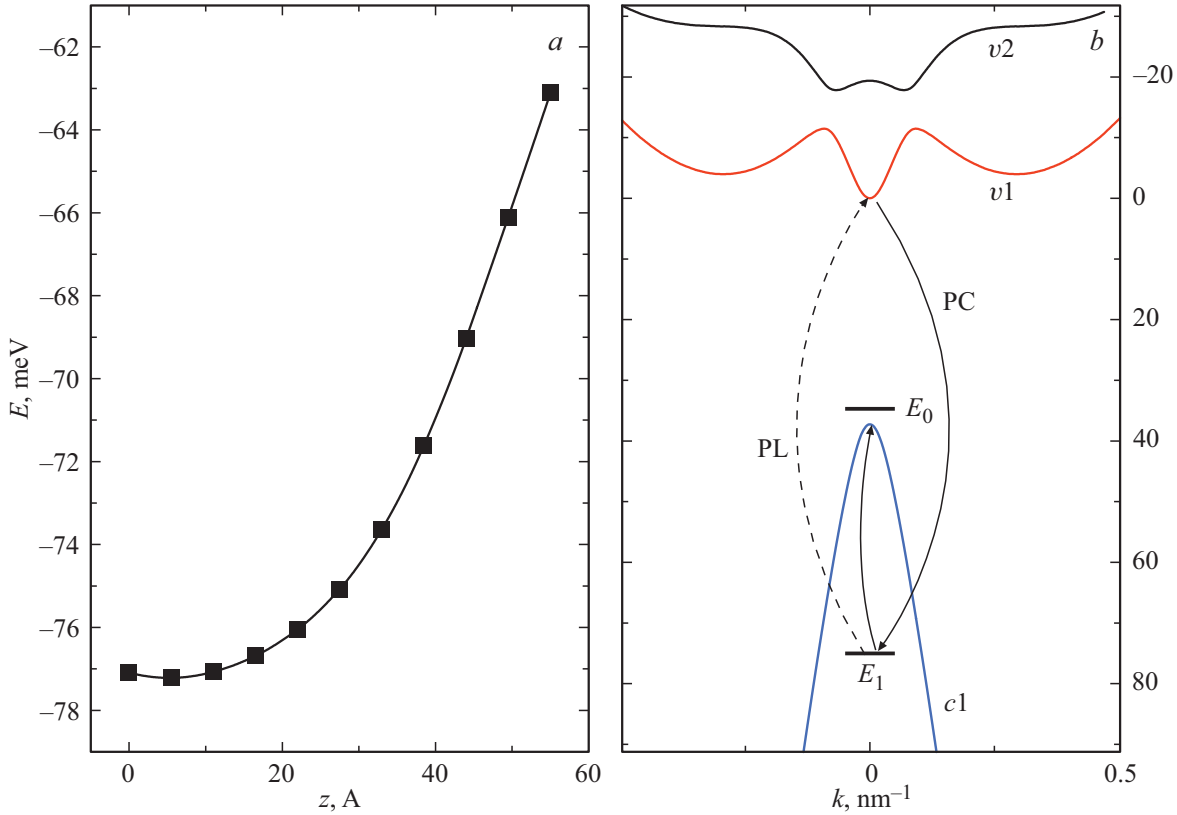

Figure 3. *a* — dependence of the ionization energy of the A_2^{-1}-center on the position in the QW; *b* — diagram for levels of mercury vacancies of centers in the structure under study. The arrows show the transitions observed in the photoluminescence and photoconductivity spectra.

conduction band (the band gap in the heterostructure is ~ 37 meV) and turns out to be resonant one. It should be noted that the ionization energy of the neutral A_2^0-center at the center of the QW is 34.7 meV, which is less than the band gap.

Figure 3, *b* shows the positions of the E_0 and E_1 levels. The distribution of mercury vacancies over charge states depends on the position of the Fermi level. Since the structure under study has an electronic type of conductivity, i.e. if the Fermi level is located near the edge of the conduction band of the quantum well of the heterostructure, then the localized, presented in the band gap states of acceptor centers are free from holes.

Thus, for the mercury vacancy in heterostructure quantum well, the situation is realized where one electron can be attached to the vacancy, but the second cannot be attached. Since the structure is of *n*-type, electrons from donor levels is larger than from acceptor centers, all divalent acceptors in the quantum well of the heterostructure will be in the charge state A_2^{-1}. Such centers participate in the formation of the photoconductivity signal: an electron, absorbing the light quantum equal to the ionization energy of the A_2^{-1}-center, passes to the acceptor state, which is resonance one. After the decay of such a resonance state, the electron finds itself in the conduction band, and the hole — in the valence band. Thus, the photoconductivity signal appears to the right of the band of interband transitions. This process is illustrated in Fig. 3, *b* by solid arrows. It should be noted that when the mercury vacancy moves into the barrier, its binding energy rapidly decreases, so their states turn out in the band gap. In the *n*-type structure, such centers are in charge states A_2^{-2} and do not participate in photoconductivity.

At the same time, both A_2^{-1}-centers in quantum wells and A_2^{-2}-centers in barriers can participate in the formation of PL. In this case, spectral bands should be observed corresponding to the ionization energy of A_2^0-centers placed in the QW of the heterostructure, and A_2^{-1}-centers located in the barrier. These energies are less than the band gap, i.e. transitions to these centers should give rise to a PL band with a quantum energy lower than that of interband transitions. In the case of equilibrium, radiative transitions with energy E_1 into the valence band are impossible, since they are due to the capture of holes on A_2^{-2}-centers in the QW, and the latter are absent in equilibrium. Nevertheless, the most intense PL line observed at low temperatures corresponds precisely to the ionization energy of the A_2^{-1}-centers placed in the QW. Such centers can arise due to nonequilibrium conditions: after the generation of electron-hole pairs in the barrier, electrons due to their high mobility rapidly diffuse and are trapped in the QW. Electron in the

QW is trapped on the resonant state of the A_2^{-1}-center, due to which fully ionized mercury vacancy will arise, after which the hole can be trapped on such A_2^{-2}-center from valence band, with the emission of the radiation quantum with energy E_1. In this case, the decay time of the resonance state of the A_2^{-2}-center due to interaction with the continuum of the conduction band should be longer than the time of the radiative transition of the hole to the center, which becomes possible due to the higher probability density of finding an electron in the resonance state (relative to other states in the conduction band) [28].

5. Suppression of Auger recombination and the possibility of obtaining SE

The results of studies of the interband PL and PC made it possible to determine the Cd concentration in the QW and its width with good accuracy. Based on the refined parameters of the structure, the threshold energy of Auger recombination was calculated, which for the main Auger process involving two electrons and a hole from the main size-quantization sub-bands was 8 meV. Studies with excitation by a pulsed CO_2 laser did not allow obtaining SE in this structure. On the other hand, it has been experimentally confirmed that SE at wavelength of $\sim 30\,\mu$m can be obtained under similar experimental conditions in structures with Auger process threshold of ~ 20 meV [10]. Note that in both cases the threshold energy is much higher than the lattice temperature 8 K (which corresponds to the energy ~ 1 meV), which should lead to strong suppression of Auger recombination if the carrier temperature is close to the lattice temperature. In particular, theoretical calculations that take the lattice and carrier temperatures to be 4.2 and 77 K, respectively, show that the mode gain parameter reaches $\sim 5000\,\mathrm{cm}^{-1}$ at a carrier concentration of $2 \cdot 10^{11}\,\mathrm{cm}^{-2}$ in structures with 20 QW, which makes it possible to depend on obtaining SE over the entire length range from 20 to $50\,\mu$m [29]. For wavelengths $\sim 30\,\mu$m, the required gain parameter for obtaining SE is much smaller and does not exceed $300\,\mathrm{cm}^{-1}$. This gain parameter is achieved [29] already at the nonequilibrium carrier concentration $\sim 6 \cdot 10^{10}\,\mathrm{cm}^{-2}$, for which, according to [30], at 8 K the probability of annihilation of an electron-hole pair due to the Auger process is still lower than the probability of radiative recombination. Thus, the absence of SE observed in the experiment in structures with threshold energy of Auger recombination < 20 meV indicates the significant difference between the carrier temperature and the lattice temperature (by more than 80 K), i.e. about the strong effect of heating. As previous studies [31,32] show, carrier heating can be reduced by transition to longer wavelength excitation, which in the wavelength range $> 10.6\,\mu$m can be implemented using QCL [33,34] provided that the threshold power density does not exceed a few $\mathrm{W/cm}^2$ [35].

6. Conclusion

In this work, an experimental study of the PC and PL spectra on the basis of which the *ex situ* characterization of the structure designed for the generation of long-wavelength radiation in the vicinity of $30\,\mu$m is carried out. Based on refined parameters, the threshold energy of Auger recombination was estimated for the structure under study, and it was shown that the possibility of obtaining SE on interband transitions is limited by carrier heating. In addition to interband transitions, features of the PC and PL spectra associated with the resonance state of the mercury vacancy are identified, and the mechanism is proposed for the appearance of the observed features under quasi-equilibrium (in the PC study mode) and nonequilibrium (in the PL study mode) conditions.

Acknowledgments

Photoconductivity studies and calculation of interband transition energies and ionization energy of acceptor states were supported by the Ministry of Science and Higher Education of the Russian Federation (grant from the President of the Russian Federation for governmental support of young Russian scientists — Candidates of Sciences and Doctors of Sciences MK-1430.2020.2). Studies of photoluminescence was supported by a grant from the Russian Science Foundation (RSF-ANR Grant # 20-42-09039).

Conflict of interest

The authors declare that they have no conflict of interest.

References

[1] L. Lunczer, P. Leubner, M. Endres, V.L. Müller, C. Brüne, H. Buhmann, L.W. Molenkamp. Phys. Rev. Lett., **123** (4), 047701 (2019).
[2] A.V. Galeeva, A.I. Artamkin, N.N. Mikhailov, S.A. Dvoretskii, S.N. Danilov, L.I. Ryabova, D.R. Khokhlov. JETP Lett., **106** (3), 162 (2017).
[3] M.V. Durnev, S.A. Tarasenko. Phys. Rev. B, **93** (7), 075434 (2016).
[4] C. Brüne, A. Roth, H. Buhmann, E.M. Hankiewicz, L.W. Molenkamp, J. Maciejko, X.-L. Qi, S.-C. Zhang. Nature Phys., **8** (6), 485 (2012).
[5] S. Ruffenach, A. Kadykov, V.V. Rumyantsev, J. Torres, D. Coquillat, D. But, S.S. Krishtopenko, C. Consejo, W. Knap, S. Winnerl, M. Helm, M.A. Fadeev, N.N. Mikhailov, S.A. Dvoretskii, V.I. Gavrilenko, S.V. Morozov, F. Teppe. APL Mater., **5** (3), 035503-1 (2017).
[6] M.S. Vitiello, G. Scalari, B. Williams, P. De Natale. Opt. Express, **23** (4), 5167 (2015).
[7] M.S. Vitiello, A. Tredicucci. Adv. Phys. X, **6** (1), 1893809 (2021).
[8] V. Rumyantsev, M. Fadeev, V. Aleshkin, N. Kulikov, V. Utochkin, N. Mikhailov, S. Dvoretskii, S. Pavlov, H.-W. Hübers, V. Gavrilenko, C. Sirtori, Z.F. Krasilnik, S. Morozov. Phys. Status Solidi B, **256** (6), 1800546 (2019).

[9] V.V. Rumyantsev, A.A. Razova, L.S. Bovkun, D.A. Tatarskiy, V.Y. Mikhailovskii, M.S. Zholudev, A.V. Ikonnikov, T.A. Uaman Svetikova, K.V. Maremyanin, V.V. Utochkin, M.A. Fadeev, V.G. Remesnik, V.Y. Aleshkin, N.N. Mikhailov, S.A. Dvoretsky, M. Potemski, M. Orlita, V.I. Gavrilenko, S.V. Morozov. Nanomaterials, **11** (7), 1855 (2021).
[10] S.V. Morozov, V.V. Rumyantsev, M.S. Zholudev, A.A. Dubinov, V.Y. Aleshkin, V.V. Utochkin, M.A. Fadeev, K.E. Kudryavtsev, N.N. Mikhailov, S.A. Dvoretskii, V.I. Gavrilenko, F. Teppe. ACS Photonics, **8** (12), 3526 (2021).
[11] V.N. Abakumov, V.I. Perel, I.N. Yassievich. *Nonradiative Recombination in Semiconductors* (North-Holland, Elsevier Science Publishers, 1991).
[12] D.N. Talwar, M. Vandevyver. J. Appl. Phys., **56** (6), 1601 (1984).
[13] V.A. Shvets, N.N. Mikhailov, D.G. Ikusov, I.N. Uzhakov, S.A. Dvoretskii. Opt. Spectrosc., **127** (2), 340 (2019).
[14] S. Dvoretsky, N. Mikhailov, Y. Sidorov, V. Shvets, S. Danilov, B. Wittman, S. Ganichev. J. Electron. Mater., **39** (7), 918 (2010).
[15] K. Jóźwikowski, M. Kopytko, A. Rogalski. J. Appl. Phys., **112** (3), 033718 (2012).
[16] D. Donetsky, G. Belenky, S. Svensson, S. Suchalkin. Appl. Phys. Lett., **97** (5), 052108 (2010).
[17] C.H. Grein, M.E. Flatté, Y. Chang. J. Electron. Mater., **37** (9), 1415 (2008).
[18] S. Krishnamurthy, M.A. Berding, Z.G. Yu. J. Electron. Mater., **35** (6), 1369 (2006).
[19] W. Lei, J. Antoszewski, L. Faraone. Appl. Phys. Rev., **2** (4), 041303 (2015).
[20] A. Rogalski. Rep. Progr. Phys., **68** (10), 2267 (2005).
[21] V.V. Rumyantsev, D.V. Kozlov, S.V. Morozov, M.A. Fadeev, A.M. Kadykov, F. Teppe, V.S. Varavin, M.V. Yakushev, N.N. Mikhailov, S.A. Dvoretskii, V.I. Gavrilenko. Semicond. Sci. Technol., **32** (9), 095007 (2017).
[22] N.N. Mikhailov, R.N. Smirnov, S.A. Dvoretsky, Y.G. Sidorov, V.A. Shvets, E.V. Spesivtsev, S.V. Rykhlitski. Int. J. Nanotechnol., **3** (1), 120 (2006).
[23] J. Shao, W. Lu, X. Lü, F. Yue, Z. Li, S. Guo, J. Chu. Rev. Sci. Instrum., **77** (6), 063104 (2006).
[24] E.G. Novik, A. Pfeuffer-Jeschke, T. Jungwirth, V. Latussek, C.R. Becker, G. Landwehr, H. Buhmann, L.W. Molenkamp. Phys. Rev. B, **72** (3), 035321 (2005).
[25] V.Y. Aleshkin, A.A. Dubinov, V.V. Rumyantsev, S.V. Morozov. J. Phys. Condens. Matter, **31** (42), 425301 (2019).
[26] D.V. Kozlov, V.V. Rumyantsev, S.V. Morozov. FTP, **53** (9), 1224 (2019) (in Russian).
[27] V.V. Rumyantsev, S.V. Morozov, A.V. Antonov, M.S. Zholudev, K.E. Kudryavtsev, V.I. Gavrilenko, S.A. Dvoretskii, N.N. Mikhailov. Semicond. Sci. Technol., **28** (12), 125007 (2013).
[28] M.S. Zholudev, V.V. Rumyantsev, S.V. Morozov. FTP, **55** (10), 861 (2021) (in Russian).
[29] A.A. Dubinov, V.V. Rumyantsev, M.A. Fadeev, V.V. Utochkin, S.V. Morozov. FTP, **55** (5), 455 (2021) (in Russian).
[30] V.Y. Aleshkin, V.V. Rumyantsev, K.E. Kudryavtsev, A.A. Dubinov, V.V. Utochkin, M.A. Fadeev, G. Alymov, N.N. Mikhailov, S.A. Dvoretsky, F. Teppe, V.I. Gavrilenko, S.V. Morozov. J. Appl. Phys., **129** (13), 133106 (2021).
[31] V.V. Rumyantsev, N.S. Kulikov, A.M. Kadykov, M.A. Fadeev, A.V. Ikonnikov, A.S. Kazakov, M.S. Zholudev, V.Ya. Aleshkin, V.V. Utochkin, N.N. Mikhailov, S.A. Dvoretsky, S.V. Morozov, V.I. Gavrilenko. FTP, **52** (11), 1263 (2018) (in Russian).
[32] V.V. Rumyantsev, M.A. Fadeev, V.Y. Aleshkin, A.A. Dubinov, V.V. Utochkin, A.V. Antonov, D.A. Ryzhov, D.I. Kuritsin, V.I. Gavrilenko, Z.F. Krasilnik, C. Sirtori, F. Teppe, N.N. Mikhailov, S.A. Dvoretsky, S.V. Morozov. J. Infrared, Millim. Terahertz Waves, **41** (7), 750 (2020).
[33] Z. Loghmari, M. Bahriz, A. Meguekam, R. Teissier, A.N. Baranov. Electron. Lett., **55** (3), 144 (2019).
[34] A.N. Baranov, M. Bahriz, R. Teissier. Opt. Express, **24** (16), 18799 (2016).
[35] V.V. Utochkin, V.Ya. Aleshkin, A.A. Dubinov, V.I. Gavrilenko, N.S. Kulikov, M.A. Fadeev, V.V. Rumyantsev, N.N. Mikhailov, S.A. Dvoretsky, A.A. Razova, S.V. Morozov. FTP, **54** (10), 1169 (2020) (in Russian).